Magyarhoni Földtani Társulat
Földtani Közlöny
Hungarian Geological Society

146/1, 47–60., Budapest, 2016

Mineralogical mosaics from the Carpathian–Pannonian region 3

Fehér, Béla[1], Szakáll, Sándor[2], Kristály, Ferenc[2], Zajzon, Norbert[2]

[1]Department of Mineralogy, Herman Ottó Museum, Kossuth u. 13., H–3525 Miskolc, Hungary
E-mail: feherbela@upcmail.hu
[2]Institute of Mineralogy and Geology, University of Miskolc, H–3515 Miskolc-Egyetemváros, Hungary

---

Ásványtani mozaikok a Kárpát–Pannon régióból 3.

Összefoglalás

Harmadik tanulmányunkban (Szakáll et al. 2013, 2014a) további mozaikszerű információkat közlünk a Kárpát–Pannon régió új ásványtani eredményeiből. Az adatokat országok és lelőhelyek szerint csoportosítottuk. Az egyes „mozaikdarabokban” az ásványok pontos leírására és — döntően XRPD, SEM-EDX és EMPA általi — meghatározására, illetve a paragenezis tömör bemutatására koncentráltunk. A tanulmányunkban szereplő ásványok olykor első említések az egész régióból vagy legalábbis az illető lelőhelyről.

Magyarországról a balatonfüredi polimetallikus ércindikációból sabelliit, a darnózseli kavicstelepből elbait, a mecseki fonolitból pektolit és sérandit, illetve az alsótelekesi evaporittelepből előkerült bazaltból zeolitok (phillipsit, kabazit) vizsgálati adatait közöljük.

Romániából a kirlibabai (Cârlibaba) ércesedésből annabergit-köttigit, míg Újmoldováról (Moldova Nouă) és Sárosdornáról (Şaru Dornei) realgár kíséretében lévő farmakolit és pikrofarmakolit jelenlétét dokumentáljuk.

Szlovákiából a korábban ismert kapkai turmalin fajbesorolását végeztük el (mikroszondás elemzés alapján magneziofoitit), kémiai és morfológiai adatokkal jellemeztük a bolgáromi (Bulhary) szodalitot, végül kimutattunk két másodlagos Ni-szulfátot (retgersit és nikkelhexahidrit) Dobsináról (Dobšiná).

Tárgyszavak: sabelliit, elbait, pektolit, sérandit, phillipsit, kabazit, farmakolit, pikrofarmakolit, magneziofoitit, szodalit, retgersit, nikkelhexahidrit

---

Abstract

This is the third paper of the authors named above (Szakáll et al. 2013, 2014a) where new, mosaic-like mineralogical data are presented from the Carpathian–Pannonian region. Data are arranged by countries and localities. Every section gives an accurate description (including XRPD, EMPA, SEM-EDX results) of the minerals and a concise description of their parageneses. Every discussed mineral is first described from the given locality and in many times even from the whole region.

From Hungary the following minerals are described: (i) sabelliite from a polymetallic ore indication at Balatonfüred, (ii) elbaite from a gravel pit at Darnózseli, (iii) pectolite and sérandite from phonolite of the Mecsek Mts, and (iv) phillipsite and chabazite from basalts found in the evaporite deposit of Alsótelekes.

From Romania the following minerals are described: (i) annabergite-köttigite solid solution from the ore deposit of Cârlibaba, and (ii) pharmacolite and picropharmacolite associated with realgar from Moldova Nouă and Şaru Dornei.

From Slovakia the following minerals are described: (i) based on EPMA results, the undetermined tourmaline from Kapka (Remetské Hámre) is classified as magnesiofoitite, a (ii) chemical and morphological description of sodalite from Bulhary, and (iii) two secondary Ni sulphates, retgersite and nickelhexahydrite, from the Co-Ni ore deposit of Dobšiná.

Keywords: sabelliite, elbaite, pectolite, sérandite, phillipsite, chabazite, pharmacolite, picropharmacolite, magnesiofoitite, sodalite, retgersite, nickelhexahydrite.

Experimental methods and samples

X-ray powder diffraction patterns of sabelliite, pharmacolite, picropharmacolite, retgersite and nickelhexahydrite were recorded on a Bruker D8 Advance diffractometer using Cu$K\alpha$ radiation (40 kV and 40 mA) with a 250-mm-radius goniometer; this was carried out in parallel-beam geometry obtained by Goebel-mirror optics, 0.25° primary axial Soller with a 0.6-mm exit slit and position sensitive Våntec-1 detector (1° opening). Samples of 1 to 5 mg were ground in agate mortar under acetone and loaded on low-background (Si crystal) sample holders. All patterns were recorded in the 2–70° (2Θ) range with a 0.007° (2Θ) / 4 second scanning rate.

X-ray diffraction studies were also performed with a 114.6 mm diameter Gandolfi camera for köttigite-annabergite and pectolite. The analytical parameters included: Cu$K\alpha$ radiation, Ni filter, 40 kV accelerating voltage, 25 mA tube current, with exposition times between 47 to 48 hours. Unit cell parameters were calculated with the UnitCell software (HOLLAND & REDFERN 1997). NIST SRM 640 silicon powder was used as an external standard for the correction of film shrinkage.

Scanning electron microscopy (SEM) studies, energy-dispersive X-ray spectroscopy (EDX), and X-ray mapping and electron microprobe measurements (EMPA) were done on a JEOL JXA-8600 Superprobe unit equipped with three wavelength-dispersive spectrometers and an EDX silicon drift detector (SDD). These examinations were carried out at the Institute of Mineralogy and Geology, University of Miskolc. For the EDX measurements 15–20 kV accelerating voltage was used, with a probe current of 10–20 nA. A 4×5 µm area was scanned with focused beam during the analyses (a stopped focused beam was used if the target area was too small).

Some minerals (elbaite, pectolite, phillipsite, chabazite and magnesiofoitite) were analyzed in wavelength-dispersive mode. Operating conditions were as follows: accelerating voltage 15 kV, probe current 20 nA, final beam diameter was 1 µm for magnesiofoitite and 10 µm for the other minerals; peak count-times were 10 s and background count-times were 5 s. The analytical standards were: quartz (Si), corundum (Al), ilmenite (Ti, Fe), olivine (Mg), augite (Ca), MnS_2 (Mn), anorthoclase (Na), microcline (K) and fluorite (F). Raw intensity data were corrected using a PAP matrix correction.

Quantitative electron microprobe analyses were also performed at the Geological Institute of Dionýz Štúr, Bratislava, Slovakia. For the analyses of sabelliite, sérandite-pectolite, köttigite-annabergite and sodalite, a Cameca SX-100 instrument was used in wavelength-dispersive mode. Operating conditions were as follows: accelerating voltage 15 kV, and probe current 20 nA. The analytical standards were: apatite (P), GaAs (As), stibnite (Sb), orthoclase (Si, K), TiO_2 (Ti), UO_2 (U), Al_2O_3 (Al), pure Cr (Cr), fayalite (Fe), forsterite (Mg), wollastonite (Ca), rhodonite (Mn), pure Co (Co), pure Ni (Ni), pure Cu (Cu), willemite (Zn), $SrTiO_3$ (Sr), baryte (S, Ba), $PbCO_3$ (Pb), albite (Na), LiF (F), and NaCl (Cl). Raw intensity data were corrected using a PAP matrix correction.

In situ determination of the Li and Be content of Darnózseli elbaite was performed by laser ablation inductively-coupled plasma mass spectrometry (LA-ICP-MS) at the Institute of Chemistry, Eötvös Loránd University, Budapest, Hungary, This involved the use of a Thermo Scientific Element 2 mass-spectrometer equipped with a New Wave UP213 laser ablation head. Measurement parameters were as follows: 213 nm laser, 55 µm spot-size, 10 Hz frequency, 0.121 mJ/impulse energy, 0.85 l/min Ar auxiliary gas, 1.3 l/min Ar carrier gas, NIST 610 and 612 standards, and Li^7 and Be^9 measured isotopes with an Al^{27} internal standard for ablation correction.

All the investigated samples are deposited in the mineral collection of the Herman Ottó Museum, Miskolc, Hungary.

Results

Hungary

Sabelliite from Balatonfüred

Sabelliite — $Cu_2Zn(AsO_4, SbO_4)(OH)_3$ — was first described from the oxidation zone of the Is Murvonis mine (Iglesias mining area, Sardinia, Italy) by OLMI et al. (1995) as an alteration product of tetrahedrite. It was associated with azurite and malachite.

The polymetallic ore indication in the Lower Triassic dolomite of the "Hajógyár" quarry at Balatonfüred — with dominant chalcopyrite, galena and smaller amounts of sphalerite and secondary chalcocite — was first described by PAPP & MÁNDY (1955). Azurite, malachite and cerussite were mentioned as alteration products of the sulphide minerals. The new samples considere in the presnet study contain tetrahedrite nests with an alteration product quite different from those described earlier. The new phase, sabelliite, appears as light blue encrustations or spherical-botryoidal aggregates. The crusts are built up of 1–3-µm-sized lamellae (*Figure 1*) according to SEM. The crust is formed above a smectite layer coating of the host rock, and shows a transition from a fine-grained mixture of phases of the inner part, to the lamellar, coarser grained outer layer. The texture suggests a supergene alteration origin of the assemblage. Sabelliite is associated with azurite and a poorly-crystallized Cu arsenate. XRD data are presented in *Table I*. The differences between peak intensities of the measured and reference patterns are attributed to a contaminated sample; this is because the specimen was mixed with dolomite, azurite and quartz. The cell parameters of

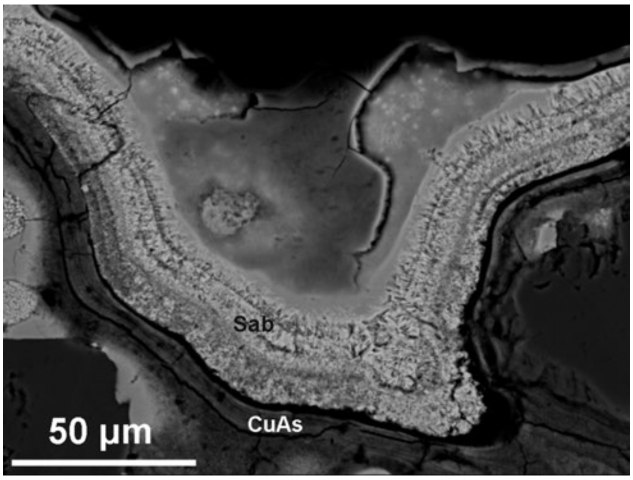

Figure 1. Sabelliite (Sab) encrustation consisting of minute scales, surrounded by poorly crystallized Cu arsenates (CuAs). Hajógyár Quarry, Balatonfüred. BSE image

1. ábra. *Sabelliit (Sab) parányi pikkelyekből álló bekérgezése rosszul kristályos Cu-arzenátokkal (CuAs) körülvéve. Balatonfüred, Hajógyári kőfejtő. BSE-kép*

Table I. X-ray powder diffraction data of sabelliite from Balatonfüred in comparison with the corresponding reflections of the ICDD 00-048-1891 card

I. táblázat. *A balatonfüredi sabelliit röntgen-pordiffrakciós adatai, összehasonlítva az ICDD 00-048-1891 kártya megfelelő reflexióival*

Sabelliite Balatonfüred		Sabelliite (ICDD 00-048-1891) Is Murvonis mine, Italy				
d (Å)	*I* (%)	*d* (Å)	*I* (%)	*h*	*k*	*l*
7.315	13	7.33	42	0	0	1
7.102	24	7.15	7	1	0	0
5.096	<1	5.11	18	1	0	1
4.101	51	4.11	55	1	1	0
3.658	37	3.66	52	0	0	2
3.577	27	3.58	49	1	1	1
3.252	5	3.25	31	1	0	2
3.195	11	3.20	46	2	0	1
2.729	6	2.726	29	1	1	2
2.684	23	2.688	29	1	2	0
2.548	31	2.548	15	0	2	2
2.520	100	2.522	100	1	2	1
2.367	8	2.369	26	0	3	0
2.252	<1	2.253	28	0	3	1
2.164	16	2.166	88	1	2	2
2.096	0	2.096	25	1	1	3
2.050	1	2.054	12	2	2	0
1.974	3	1.974	18	2	2	1
1.902	1	1.901	18	3	1	1
1.829	1	1.828	7	0	0	4
1.805	9	1.805	92	1	2	3
1.734	1	1.733	23	1	3	2
1.725	4	1.725	23	0	4	1
1.670	1	1.670	26	1	1	4
1.626	4	1.626	18	2	0	4
1.590	2	1.591	22	3	2	1
1.569	<1	1.569	9	2	2	3
1.550	34	1.550	100	4	1	0
1.532	5	1.532	8	3	1	3
1.511	7	1.513	85	1	2	4
1.488	1	1.489	17	3	2	2
1.463	5	1.462	11	0	0	5
1.447	1	1.448	16	0	3	4

Table II. Electron-microprobe data of sabelliite from Balatonfüred (in wt%)

II. táblázat. *A balatonfüredi sabelliit elektronmikroszondás elemzési adatai tömegszázalékban*

	1	2	3	Average Átlag
SO_3	0.05	0.05	0.05	0.05
As_2O_5	23.76	18.12	19.83	20.57
Sb_2O_5	5.68	7.29	6.94	6.64
SiO_2	0.87	1.50	0.60	0.99
CuO	39.82	37.11	40.12	39.02
ZnO	21.03	29.47	22.86	24.45
H_2O	n.d.	n.d.	n.d.	*6.77
Total	91.22	93.52	90.40	98.49

n.d. = not determined / *nincs meghatározva.*

* Calculated from stoichiometry / *A sztöchiometrikus összetételből számolva: OH = 3 apfu.*

sabelliite calculated from the measured XRD data are a = 8.201 Å, c = 7.315 Å, and V = 426.068 Å^3. Three electron microprobe analyses were performed on sabelliite (*Table II*). The chemical formula, based on the average of the microprobe data, is:

$Cu_{1.96}Zn_{1.20}(As_{0.72}Sb_{0.16}Si_{0.07})_{\Sigma=0.95}O_4(OH)_3$.

Zeolites from basalt, Alsótelekes

In the Bódva Valley (NE Hungary), Triassic ophiolites built up from serpentinites, gabbros (metagabbros) and tholeiitic basalts (metabasalts) — probably of a lherzolitic origin — are found as remnants of an oceanic floor. Fragmented blocks of the ophiolites, 1 to several 100 m in size, are embedded in Permian evaporites, as a result of tectonic processes. The serpentinite has a unique mineral paragenesis with most probably, an ocean-floor metasomatic overprint (ZAJZON et al. 2013). At the Alsótelekes evaporite mine, dm-sized blocks of strongly-weathered serpentinite and basalt are known; these are mainly from the debris of the industrial road (surrounded by excavations) and the waste-pile, respectively (ZELENKA et al. 2005). Zeolites (chabazite and phillipsite) and carbonates (aragonite and calcite) fill the voids of the amygdaloidal basalts. Zeolites are sometimes coated by smectite. Chabazite forms 0.1 mm-sized rhombohedra, while the phillipsite aggregates consist of 0.1–0.3 mm-sized fourlings. The latter are mainly hollow skeletal crystals with partially developed faces (*Figure 2*). According to the electron-microprobe analyses (*Tables III* and *IV*) both zeolites are potassium-dominant, i.e. chabazite-K and phillipsite-K. For these zeolite minerals a "balance error" E was calculated from the electron microprobe analyses (see PASSAGLIA 1970): $E = [(Al + Fe^{3+} - Al_{theor})/Al_{theor}]\times100$, where $Al_{theor} = Na + K + 2(Ca + Mg + Sr + Ba)$. A zeolite analysis is considered reliable, if the balance error is less than ± 10%.

It is worth mentioning that, after potassium (0.42–0.51

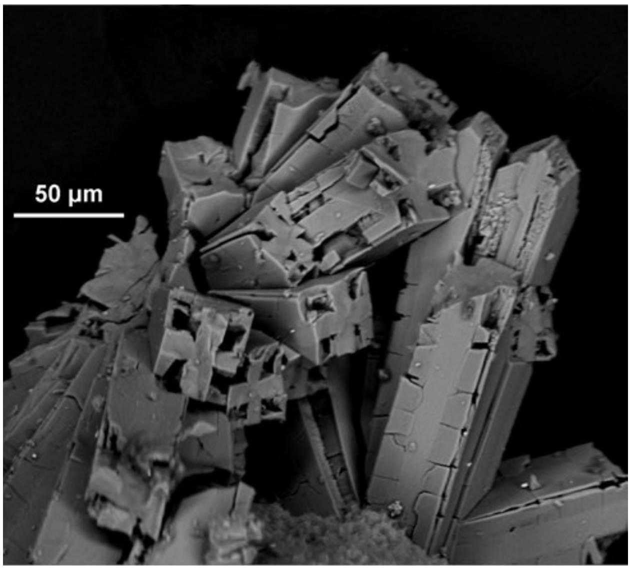

Figure 2. Phillipsite-K, skeletal fourlings from Alsótelekes. BSE image

2. ábra. *Phillipsit-K vázkristályos megjelenésű négyes ikrei. Alsótelekes. BSE-kép*

Table III. Electron-microprobe data of chabazite from Alsótelekes (in wt%)

III. táblázat. *Az alsótelekesi kabazit elektronmikroszondás elemzési adatai tömegszázalékban*

SiO_2	58.61	57.13	58.70	58.32	58.94	57.40
Al_2O_3	16.49	16.33	16.06	15.62	16.26	15.82
Fe_2O_3	0.07	0.06	0.09	0.04	0.00	0.02
MgO	2.70	2.52	2.80	2.61	2.70	2.90
CaO	2.49	2.48	2.49	2.54	2.18	2.20
BaO	0.00	0.02	0.05	0.00	0.02	0.00
Na_2O	0.13	0.18	0.17	0.15	0.12	0.19
K_2O	5.24	4.54	4.30	4.96	4.73	4.63
Total	85.74	83.26	84.66	84.25	84.96	83.15
Cation numbers based on 12 oxygens Kationszámok 12 oxigénre						
Si	4.49	4.49	4.53	4.54	4.53	4.51
Al	1.49	1.51	1.46	1.43	1.47	1.47
Fe	0.00	0.00	0.01	0.00	0.00	0.00
Mg	0.31	0.30	0.32	0.30	0.31	0.34
Ca	0.20	0.21	0.21	0.21	0.18	0.19
Ba	0.00	0.00	0.00	0.00	0.00	0.00
Na	0.02	0.03	0.03	0.02	0.02	0.03
K	0.51	0.46	0.42	0.49	0.46	0.46
E (%)	-3.87	0.00	-2.65	-6.54	0.68	-5.16
R	0.75	0.75	0.76	0.76	0.76	0.75

E: balance error / *egyensúlyi hiba.*
R = Si/(Si + Al + Fe).

Table IV. Electron-microprobe data of phillipsite from Alsótelekes (in wt%)

IV. táblázat. *Az alsótelekesi phillipsit elektronmikroszondás elemzési adatai tömegszázalékban*

SiO_2	56.14	51.66	52.49	55.33	56.12
Al_2O_3	16.95	18.02	18.35	17.41	17.05
Fe_2O_3	0.09	0.22	0.00	0.08	0.09
MgO	0.00	0.00	0.00	0.00	0.08
CaO	5.05	6.27	5.95	5.28	5.32
BaO	1.82	1.10	1.23	1.65	1.50
Na_2O	0.72	0.70	0.62	0.65	0.70
K_2O	6.51	6.32	6.50	6.13	5.92
Total	87.27	84.30	85.14	86.55	86.78
Cation numbers based on 32 oxygens Kationszámok 32 oxigénre					
Si	11.72	11.22	11.27	11.62	11.71
Al	4.17	4.61	4.64	4.31	4.19
Fe	0.01	0.04	0.00	0.01	0.01
Mg	0.00	0.00	0.00	0.00	0.02
Ca	1.13	1.46	1.37	1.19	1.19
Ba	0.15	0.09	0.10	0.14	0.12
Na	0.29	0.29	0.26	0.26	0.28
K	1.73	1.75	1.78	1.64	1.58
E (%)	-8.73	-9.53	-6.83	-5.26	-7.08
R	0.74	0.71	0.71	0.73	0.74

E: balance error / *egyensúlyi hiba.*
R = Si/(Si + Al + Fe).

apfu), the second most abundant extra-framework cation of chabazite is magnesium (0.30–0.34 apfu), although the calcium content is also significant (0.18–0.21 apfu). Phillipsite also has a mixed extra-framework cation content: K (1.58–1.78 apfu) > Ca (1.13–1.46 apfu) > Na (0.26–0.29 apfu) > Ba (0.09–0.15 apfu), with a negligible amount of magnesium.

Pectolite and sérandite from phonolite, Hosszúhetény

The miarolitic cavities of phonolite at Hosszúhetény – in conformity with the alkaline character of the rock – are rich in Na-containing silicates. The latter include, for example the common natrolite, analcime, albite, sanidine or the less common thomsonite, apophyllite, sodalite, eudialyte and neptunite (SZAKÁLL et al. 2014b). A rarer member of this assemblage is pectolite, which usually forms 0.5–1 mm-sized, elongated laths and acicular crystals; these are scattered or grouped into radial aggregates on analcime. Analcime sometimes overgrows the radial aggregates. Pectolite was formed as a hydrothermal alteration product of rock-forming minerals like nepheline and plagioclase. Its X-ray powder diffraction data are given in *Table V.* The differences between peak intensities of the measurements

Table V. X-ray powder diffraction data of pectolite from Hosszúhetény compared with the data of the ICDD 00-033-1223 card

V. táblázat. *A hosszúhetényi pektolit röntgen-pordiffrakciós adatai, összehasonlítva az ICDD 00-033-1223 kártya adataival*

Pectolite Hosszúhetény		Pectolite (ICDD 00-033-1223) Ledalfoot, Ayrshire, Scotland		
d (Å)	*I* (%)	*d* (Å)	*I* (%)	*hkl*
7.80	10	7.76	2	100
6.99	10	6.98	4	001
5.75	5	5.81	1	-110
5.47	12	5.45	5	-101
4.99	1	4.967	1	101
4.65	3	4.656	2	110
		4.573	2	-111
		4.371	1	1-11
4.03	10	4.028	4	11-1
3.889	23	3.883	10	200
3.752	6	3.750	2	-210, 111
3.506	16	3.499	11	002
3.422	9	3.419	5	-211
3.316	36	3.307	16	-102
3.270	25	3.268	15	201
3.160	21	3.154	12	0-12
3.087	60	3.082	40	102, 012
		3.061	20	-112
2.916	100	2.901	100	120, -220
2.736	28	2.746	7	12-1
		2.732	13	-202, -221
2.630	5	2.622	3	-310
2.593	22	2.591	12	300
2.493	3	2.486	1	0-22, 202
		2.467	1	2-12, -122
2.440	14	2.433	8	1-22
2.416	10	2.417	7	022
		2.360	2	301
2.334	14	2.330	11	220, -320

Table V cont.

V. táblázat. *folyt.*

Pectolite Hosszúhetény		Pectolite (ICDD 00-033-1223) Ledalfoot, Ayrshire, Scotland		
d (Å)	*I* (%)	*d* (Å)	*I* (%)	*d* (Å)
2.298	21	2.308	1	12-2
		2.295	10	-103, -222
2.267	3	2.266	1	310
2.228	3	2.228	2	0-13, 212
		2.219	2	31-1
2.168	20	2.164	15	3-21, 221
2.089	3	2.089	3	-203
		2.078	3	2-31
		2.052	1	-213
2.018	4	2.013	4	22-2
1.998	5	1.996	5	-322, 302
		1.989	4	-410
		1.957	1	-411, 0-23
1.948	6	1.944	4	1-32, 400
1.920	3	1.920	1	-401, 1-23
		1.904	1	023
1.884	9	1.888	3	032
		1.878	6	3-22, -232
1.862	2	1.863	1	-223
1.831	10	1.833	2	2-32
		1.828	6	401, 13-2
1.761	20	1.757	30	-140, 004
1.718	14	1.728	4	-332
		1.715	8	32-2, 22-3
1.707	10	1.708	9	-422, -323
1.677	2	1.674	1	104
1.659	6	1.656	3	303, -204
		1.617	1	-233
1.604	6	1.602	4	4-22, 322
1.565	7	1.566	5	-403, -142
1.553	10	1.558	5	0-42, 500
1.543	5	1.549	6	-520, -242
1.530	5	1.528	3	32-3
1.521	3	1.520	4	042, -423
1.491	10	1.4876	7	501
1.473	10	1.4696	7	2-24
1.463	8	1.4615	5	124
1.443	2	1.4560	4	240, -440
1.433	2	1.4379	3	3-42
		1.4320	2	142
1.404	1	1.4097	1	0-34
		1.4006	2	0-43, -134
1.392	3	1.3901	3	304
1.376	6	1.3740	6	24-2, 502
1.356	3	1.3662	3	-404, -442
		1.3539	4	-503
		1.3397	1	-343, 32-4
		1.3297	1	-424
		1.3208	1	-351
1.313	2	1.3100	3	1-52
1.299	4	1.2961	5	-601
		1.2838	1	-305
1.270	1	1.2679	2	5-41, 341
		1.2590	1	-450
1.249	3	1.2455	2	1-44
1.237	2	1.2348	1	-144

and the reference patterns are attributed to the different measurement geometries: i.e. Gandolfi for the Hungarian sample and Bragg-Brentano for the reference sample. Least-squares refinement of the XRD data using the program UnitCell (HOLLAND & REDFERN 1997) on 60 indexed lines leads to a = 8.007(6), b = 6.988(8), c = 7.037(5) Å, α = 90.7(1)°, β = 95.12(8)°, γ = 102.19(8)°, V = 383.1(5) $Å^3$ unit cell parameters. Six electron microprobe analyses were performed on the cavity-filling pectolite (*Table VI*).

Some 0.1-mm-sized euhedral crystals of members of the sérandite-pectolite solid solution, $NaMn_2Si_3O_8(OH)$–$NaCa_2Si_3O_8(OH)$, were observed in a phonolite sample, where the crystals are found in the rock matrix. According to four electron microprobe point analyses, they correspond to solid-solution compositions close to the sérandite/pectolite boundary. Two of the analyses fall on the sérandite side (Mn > Ca) and the other two on the pectolite side (Ca > Mn) of the compositional field (*Table VII*). The mineral is associated with aegirine, potassium feldspar and monazite (*Figure 3*) at the Köves-tető locality. It forms subhedral crystals, developed on the potassium feldspar, which precede nepheline. The potassium feldspar presents a hydrothermal alteration pattern as structure-controlled dissolution (large number of pores); this could be related to the processes that generated the sérandite-pectolite formation. The Mn → Ca substitution in the sérandite-pectolite solid solution is well known (TAKÉUCHI et al. 1976). Both minerals are characteristic components of alkaline magmatic rocks, but up to

Table VI. Electron-microprobe data of cavity-filling pectolite from Hosszúhetény in wt%

VI. táblázat. A hosszúhetényi üregkitöltő pektolit elektron-mikroszondás elemzési adatai (tömegszázalékban)

SiO_2	56.24	55.63	54.95	56.43	54.81	54.80
Al_2O_3	0.24	0.00	0.18	0.00	0.00	0.00
Fe_2O_3	1.82	1.02	0.95	0.99	1.33	1.42
MgO	0.00	0.00	0.00	0.00	0.00	0.00
CaO	30.89	32.42	32.49	32.17	32.15	32.06
BaO	0.00	0.00	0.00	0.00	0.04	0.00
Na_2O	8.55	8.19	8.06	8.61	8.89	8.26
K_2O	0.00	0.01	0.00	0.00	0.00	0.00
H_2O*	2.75	2.73	2.72	2.77	2.73	2.72
Total	100.49	100.00	99.35	100.97	99.95	99.26
Ion numbers based on 9 oxygens Ionszámok 9 oxigénre						
Si	3.06	3.05	3.03	3.06	3.02	3.03
Al	0.02	0.00	0.01	0.00	0.00	0.00
Fe	0.07	0.04	0.04	0.04	0.06	0.06
Mg	0.00	0.00	0.00	0.00	0.00	0.00
Ca	1.80	1.90	1.92	1.87	1.90	1.90
Ba	0.00	0.00	0.00	0.00	0.00	0.00
Na	0.90	0.87	0.86	0.90	0.95	0.89
K	0.00	0.00	0.00	0.00	0.00	0.00
OH	1.00	1.00	1.00	1.00	1.00	1.00

* Calculated from stoichiometry. / *A sztöchiometrikus összetételből számolva: OH = 1 apfu.*

now in the whole Carpathian region pectolite was described only from the nepheline-syenites of the Ditrău Alkaline Massif (SZAKÁLL & KRISTÁLY 2010).

Table VII. Electron-microprobe data of sérandite-pectolite from Hosszúhetény (in wt%): (1–2) sérandite; (3–4) pectolite

VII. táblázat. *A hosszúhetényi sérandit-pektolit elegykristályok elektronmikroszondás elemzési adatai (tömegszázalékban): (1–2) sérandit; (3–4) pektolit*

	(1)	(2)	(3)	(4)
SiO_2	51.96	52.20	52.13	51.78
TiO_2	0.03	0.01	0.00	0.01
Al_2O_3	0.00	0.02	0.00	0.00
Cr_2O_3	0.01	0.00	0.00	0.00
MgO	0.00	0.00	0.00	0.02
CaO	14.59	15.14	16.56	17.74
MnO	20.75	19.67	18.92	17.82
FeO	3.09	2.63	2.41	2.12
NiO	0.01	0.00	0.00	0.01
Na_2O	8.04	8.32	8.59	8.49
K_2O	0.01	0.05	0.01	0.01
F	0.00	0.00	0.00	0.00
Cl	0.00	0.01	0.00	0.01
H_2O*	2.60	2.60	2.63	2.60
-O = F, Cl	0.00	0.00	0.00	0.00
Total	101.09	100.65	101.25	100.61
Ion numbers based on 9 anions (O, OH)** Ionszámok 9 anionra (O, OH)**				
Si	2.99	3.01	2.99	2.98
Ca	0.90	0.93	1.02	1.09
Mn	1.01	0.96	0.92	0.87
Fe	0.15	0.13	0.12	0.10
Na	0.90	0.93	0.95	0.95
OH	1.00	1.00	1.00	1.00

* Calculated from stoichiometry. / *A sztöchiometrikus összetételből számolva: OH = 1 apfu.*

** Elements with ion numbers = 0.00 (Ti, Al, Cr, Mg, Ni, K, F, Cl) are omitted. / *A 0,00 ionszámú elemeket (Ti, Al, Cr, Mg, Ni, K, F, Cl) kihagytuk.*

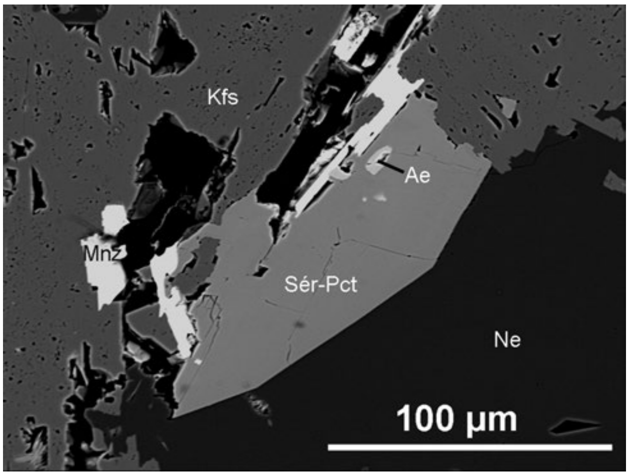

Figure 3. Sérandite-pectolite mixed crystal (Sér-Pct) with nepheline (Ne), potassium feldspar (Kfs), monazite (Mnz) and aegirine (Ae). Köves Hill, Hosszúhetény. BSE image

3. ábra. *Sérandit-pektolit elegykristály (Sér-Pct) nefelinnel (Ne), kálifölddpáttal (Kfs), monacittal (Mnz) és egirinnel (Ae). Hosszúhetény, Köves-tető. BSE-kép*

Elbaite from the Darnózseli gravel pit

Members of the tourmaline supergroup are complex borosilicate minerals with a generalized structural formula $XY_3Z_6(T_6O_{18})(BO_3)_3V_3W$, where X = Na, Ca, K or vacancy ([]); Y = Fe^{2+}, Mg, Mn^{2+}, Al, Li, Fe^{3+} or Cr; Z = Al, Fe^{3+}, Mg or Cr; T = Si, Al or B; V = OH or O; and W = OH, F or O. Tourmaline species are defined in accordance with the dominant-valency rule, such that in a relevant site the dominant ion of the dominant valence state is used for the basis of nomenclature (HENRY et al. 2011).

The sediments of the Danube River are exposed by numerous gravel pits on the Little Hungarian Plain. 1–2 mm-sized fragments or, rarely, whole crystals of pink tourmaline can sometimes be found in the sand fraction of the gravel of the pit at Darnózseli. According to the electron-microprobe analyses, this pink tourmaline is an X-site vacant elbaite. Namely the dominant cations are Na and vacancy at the X site, Al and Li at the Y site, Al at the Z site, Si at the T site, and OH at both V and W sites. At the X site, the contents of sodium, calcium and vacancy are in a fairly narrow range: Na = 0.471–0.551, Ca = 0.008–0.013 and vacancy ([]) = 0.436–0.519 apfu. Plotting the analytical values on the Na-Ca-vacancy ternary diagram (*Figure 4*), the compositions of the Darnózseli tourmaline fall on the fields of elbaite and rossmanite, near the boundary between them. At the Y site the aluminum and lithium content is considerable, while the quantity of other elements (e.g. magnesium, manganese and iron) is negligible. In *Table VIII* the calculated Li-contents are indicated — these were given from the stoichiometry, i.e. Al^Y + Ti + Mn + Mn + Fe + Li = 3.00 apfu. However, the Li-content has also been

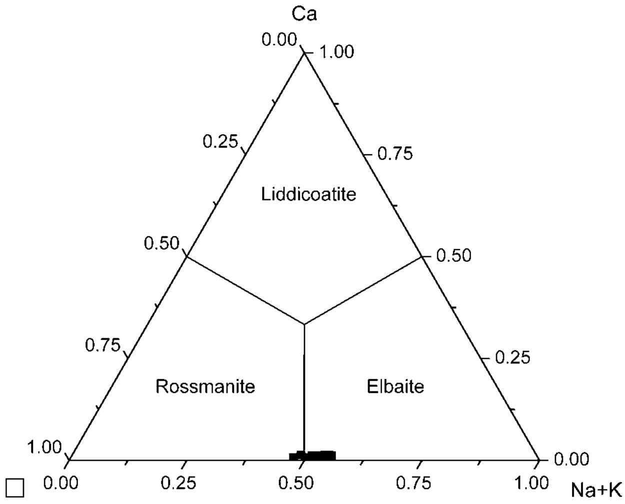

Figure 4. Chemical composition of the tourmaline of Darnózseli plotted in the Na-Ca-vacancy ([]) ternary diagram of Li-tourmalines

4. ábra. *A darnózseli turmalin kémiai összetétele a Li-turmalinok Na-Ca-kationhiány ([]) háromszögdiagramjában ábrázolva*

Table VIII. Electron-microprobe data of tourmaline from Darnózseli (in wt%)

***VIII. táblázat.** A darnózseli turmalin elektronmikroszondás elemzési adatai tömegszázalékban*

	(1)	(2)	(3)	(4)	(5)	(6)	(7)	(8)	(9)	(10)	(11)	(12)	(13)	(14)
SiO_2	37.19	37.12	37.01	37.00	37.85	37.86	37.37	37.37	36.75	37.00	37.14	36.74	37.08	37.55
TiO_2	0.00	0.00	0.00	0.00	0.00	0.00	0.00	0.01	0.00	0.01	0.00	0.00	0.00	0.02
B_2O_3*	11.17	11.11	11.10	11.14	11.27	11.30	11.09	11.13	11.08	11.12	11.13	11.06	11.11	11.16
Al_2O_3	43.83	43.34	43.47	43.74	43.93	44.25	43.04	43.15	43.60	43.48	43.50	43.38	43.50	43.31
FeO**	0.01	0.00	0.00	0.00	0.00	0.00	0.00	0.00	0.03	0.00	0.00	0.15	0.00	0.00
MgO	0.04	0.00	0.04	0.00	0.03	0.03	0.00	0.03	0.00	0.00	0.01	0.00	0.00	0.03
CaO	0.07	0.08	0.07	0.08	0.05	0.05	0.08	0.06	0.07	0.07	0.08	0.08	0.07	0.07
MnO	0.20	0.18	0.00	0.23	0.08	0.00	0.17	0.28	0.12	0.30	0.23	0.26	0.08	0.10
Li_2O*	1.82	1.87	1.86	1.84	1.88	1.86	1.86	1.88	1.82	1.85	1.85	1.81	1.87	1.89
Na_2O	1.68	1.78	1.74	1.80	1.66	1.58	1.60	1.82	1.73	1.81	1.76	1.74	1.75	1.70
K_2O	0.02	0.02	0.01	0.01	0.01	0.01	0.00	0.00	0.01	0.02	0.02	0.03	0.02	0.01
F	0.07	0.00	0.04	0.01	0.06	0.00	0.00	0.03	0.00	0.06	0.01	0.06	0.00	0.00
H_2O*	3.82	3.83	3.81	3.84	3.86	3.90	3.83	3.83	3.82	3.81	3.84	3.79	3.83	3.85
-O=F	0.03	0.00	0.02	0.00	0.03	0.00	0.00	0.01	0.00	0.03	0.00	0.03	0.00	0.00
Total	99.90	99.33	99.13	99.69	100.66	100.85	99.04	99.58	99.03	99.49	99.57	99.07	99.31	99.69
Structural formulae based on 31 anions (O, OH, F) Szerkezeti képlet 31 (O, OH, F) anionra														
Si	5.786	5.807	5.796	5.771	5.835	5.822	5.856	5.834	5.767	5.785	5.798	5.772	5.799	5.846
Al	0.214	0.193	0.204	0.229	0.165	0.178	0.144	0.166	0.233	0.215	0.202	0.228	0.201	0.154
ΣT	**6.000**	**6.000**	**6.000**	**6.000**	**6.000**	**6.000**	**6.000**	**6.000**	**6.000**	**6.000**	**6.000**	**6.000**	**6.000**	**6.000**
B	**3.000**	**3.000**	**3.000**	**3.000**	**3.000**	**3.000**	**3.000**	**3.000**	**3.000**	**3.000**	**3.000**	**3.000**	**3.000**	**3.000**
Al	6.000	6.000	6.000	6.000	6.000	6.000	6.000	6.000	6.000	6.000	6.000	6.000	6.000	6.000
ΣZ	**6.000**	**6.000**	**6.000**	**6.000**	**6.000**	**6.000**	**6.000**	**6.000**	**6.000**	**6.000**	**6.000**	**6.000**	**6.000**	**6.000**
Al	1.822	1.799	1.820	1.813	1.817	1.841	1.804	1.774	1.831	1.798	1.803	1.805	1.816	1.794
Ti	0.000	0.000	0.000	0.000	0.000	0.000	0.000	0.001	0.000	0.001	0.000	0.000	0.000	0.002
Mg	0.009	0.000	0.009	0.000	0.007	0.007	0.000	0.007	0.000	0.000	0.002	0.000	0.000	0.007
Mn	0.026	0.024	0.000	0.030	0.010	0.000	0.023	0.037	0.016	0.040	0.030	0.035	0.011	0.013
Fe^{2+}	0.001	0.000	0.000	0.000	0.000	0.000	0.000	0.000	0.004	0.000	0.000	0.020	0.000	0.000
Li	1.141	1.177	1.170	1.157	1.166	1.152	1.173	1.181	1.149	1.161	1.165	1.141	1.173	1.184
ΣY	**3.000**	**3.000**	**3.000**	**3.000**	**3.000**	**3.000**	**3.000**	**3.000**	**3.000**	**3.000**	**3.000**	**3.000**	**3.000**	**3.000**
Ca	0.012	0.013	0.012	0.013	0.008	0.008	0.013	0.010	0.012	0.012	0.013	0.013	0.012	0.012
Na	0.507	0.540	0.528	0.544	0.496	0.471	0.486	0.551	0.526	0.549	0.533	0.530	0.531	0.513
K	0.004	0.004	0.002	0.002	0.002	0.002	0.000	0.000	0.002	0.004	0.004	0.006	0.004	0.002
[]	0.478	0.443	0.458	0.440	0.494	0.519	0.500	0.439	0.460	0.436	0.450	0.450	0.454	0.473
ΣX	**1.000**	**1.000**	**1.000**	**1.000**	**1.000**	**1.000**	**1.000**	**1.000**	**1.000**	**1.000**	**1.000**	**1.000**	**1.000**	**1.000**
OH	3.966	4.000	3.980	3.995	3.971	4.000	4.000	3.985	4.000	3.970	3.995	3.970	4.000	4.000
F	0.034	0.000	0.020	0.005	0.029	0.000	0.000	0.015	0.000	0.030	0.005	0.030	0.000	0.000

* Calculated from stoichiometry. / *A sztöchiometrikus összetételből számolva.*

** Total Fe was regarded as FeO. / *Az összes vasat FeO-ként vettük figyelembe.*

determined directly by LA-ICP-MS, but the measured Li_2O quantities are rather low (0.95–1.40 wt%) as compared to the calculated values (1.81–1.89 wt%). Be content, determined by LA-ICP-MS, is between 20–80 ppm with an average of 60 ppm. The pink elbaite crystals in the Danube sediments could be derived from the pegmatites of the Moravian Massif in the Czech Republic. The most likely locality is Rožná, where the lepidolite subunit and quartz core of a large lepidolite-subtype pegmatite dike contain *X*-site vacant elbaite (NOVÁK & SELWAY 1997) with a chemistry very similar to that of the Darnózseli tourmaline.

Romania

Köttigite–annabergite solid solution from Cârlibaba (Kirlibaba)

Many secondary mineral phases can be found on the historical dumps of the polymetallic mineralization located in the vicinity of the town of Cârlibaba (Zepharovich 1859). Here we report for the first time 20–30-μm-sized, stubby, prismatic crystals of köttigite–annabergite: $Zn_3(AsO_4)_2 \bullet 8H_2O - Ni_3(AsO_4)_2 \bullet 8H_2O$. The measured XRD data are presented in *Table IX.* Least squares refinement of the XRD data using the program UnitCell (Holland & Redfern 1997) on 36 indexed lines leads to $a = 10.117(4)$, $b = 13.429(4)$, $c = 4.762(2)$ Å, $\beta = 101.99(4)°$, and $V = 632.8(3)$ Å^3. The measured EPMA data are listed in *Table X.*

Table IX. X-ray powder diffraction data of köttigite-annabergite from Cârlibaba compared with the corresponding reflections of the ICDD 00-033-1467 card

IX. táblázat. *A kirlibabai (Cârlibaba) köttigit-annabergit röntgen-pordiffrakciós adatai, összehasonlítva az ICDD 00-033-1467 kártya megfelelő reflexióival*

Köttigite Cârlibaba		Synthetic köttigite ICDD 00-033-1467				
d (Å)	*I* (%)	*d* (Å)	*I* (%)	*h*	*k*	*l*
7.97	47	7.97	24	1	1	0
6.71	100	6.72	100	0	2	0
4.94	13	4.951	10	2	0	0
4.60	3	4.595	5	-1	0	1
4.40	22	4.403	14	0	1	1
4.08	5	4.083	9	1	3	0
3.988	3	3.987	6	2	2	0
3.915	15	3.923	15	1	0	1
3.664	8	3.660	7	-2	1	1
3.221	38	3.229	47	0	3	1
3.005	46	3.013	34	2	1	1
		3.002	36	-3	0	1
2.780	7	2.779	8	2	4	0
2.741	27	2.736	28	-3	2	1
2.710	21	2.711	25	-1	4	1
2.657	13	2.657	16	3	3	0
2.548	7	2.549	9	1	4	1
2.459	16	2.468	16	3	0	1
2.331	14	2.343	10	-1	1	2
		2.328	22	0	5	1
2.239	4	2.238	5	0	6	0
2.196	7	2.200	4	0	2	2
		2.195	9	-2	5	1
2.083	9	2.0838	11	3	5	0
2.014	1	2.0120	2	-1	6	1
1.987	3	1.9874	2	3	4	1
1.953	8	1.9594	8	5	1	0
		1.9542	8	1	3	2
1.915	8	1.9153	3	-3	3	2
1.839	2	1.8434	7	4	3	1
1.789	2	1.7893	3	-4	5	1
1.774	2	1.7744	2	0	7	1
1.691	5	1.6884	9	1	5	2
1.681	7	1.6789	11	0	8	0
1.662	7	1.6643	11	-3	5	2
		1.6604	10	4	6	0
1.615	3	1.6154	3	4	5	1
1.603	3	1.6023	2	6	2	0
1.593	2	1.5941	1	5	5	0
1.562	2	1.5621	3	-6	3	1
1.542	2	1.5441	2	1	8	1

Table X. Electron-microprobe data of annabergite (1-2) and köttigite (3-4) from Cârlibaba, Romania (in wt%)

X. táblázat. *Annabergit (1-2) és köttigit (3-4) elektronmikroszondás elemzési adatai, Kirlibaba (Cârlibaba), Románia (tömegszázalékban)*

	(1)	(2)	(3)	(4)
SO_3	0.06	0.06	0.07	0.04
P_2O_5	0.00	0.04	0.00	0.01
As_2O_5	41.71	42.36	41.47	45.70
SiO_2	0.20	0.15	0.09	0.17
UO_2	0.00	0.00	0.02	0.03
Al_2O_3	0.12	0.08	0.00	0.00
Fe_2O_3	0.12	0.22	0.06	0.25
MgO	0.56	0.46	0.13	0.10
CaO	0.18	0.11	0.02	0.07
MnO	3.39	4.91	1.47	1.51
CoO	14.52	14.65	1.87	1.42
NiO	20.70	16.01	1.67	1.65
CuO	0.20	0.11	0.36	0.31
ZnO	2.82	6.23	39.81	41.39
SrO	0.04	0.00	0.01	0.00
BaO	0.00	0.00	0.00	0.00
PbO	0.06	0.01	0.04	0.02
Total	84.68	85.40	87.09	92.67
Cation numbers based on 8 oxygens Kationszámok 8 oxigénre				
S	0.00	0.00	0.00	0.00
P	0.00	0.00	0.00	0.00
As	1.88	1.90	1.95	2.00
Si	0.02	0.01	0.01	0.01
U	0.00	0.00	0.00	0.00
Al	0.01	0.01	0.00	0.00
Fe	0.01	0.01	0.00	0.02
Mg	0.07	0.06	0.02	0.01
Ca	0.02	0.01	0.00	0.01
Mn	0.25	0.36	0.11	0.11
Co	0.94	0.94	0.13	0.09
Ni	1.44	1.10	0.12	0.11
Cu	0.01	0.01	0.02	0.02
Zn	0.18	0.39	2.64	2.56
Sr	0.00	0.00	0.00	0.00
Ba	0.00	0.00	0.00	0.00
Pb	0.00	0.00	0.00	0.00

Even though Sturman (1976) described köttigite–parasymplesite solid solution from the Ojuela mine (Mexico), Jambor & Dutrizac (1995) recorded synthetic annabergite–erythrite–hörnesite solid solutions, and Zajzon et al. (2015) mentioned annabergite–erythrite–(Co-Fe-Ni-Ca) arsenates from Avram Iancu, Romania. Minerals corresponding to the köttigite–annabergite have not been described yet.

Pharmacolite and picropharmacolite from Moldova Nouă (Újmoldova) and pharmacolite from Şaru Dornei (Sárosdorna)

The formation of arsenates is connected to realgar mineralizations at both localities. Realgar and orpiment are well known minerals of the polymetallic ore deposits at Moldova Nouă (Rădulescu & Dimitrescu 1966). Rare arsenates were found in the nests and voids of As sulphides located in vein-filling calcite. Colourless, 0.5–2-mm-sized, elongated laths of pharmacolite and picropharmacolite form radial aggregates and crusts (*Figure 5*). The X-ray powder diffraction pattern of picropharmacolite is shown in *Figure 6*. The identification of minerals is confirmed by the EDX spectra: Ca and As were detected in one of the minerals that can be considered as pharmacolite — ideally $Ca(HAsO_4) \cdot 2H_2O$ — while Ca, As and Mg were detected in the other mineral that corresponds to picropharmacolite, ideally $Ca_4Mg(AsO_4)_2(HAsO_3OH)_2 \cdot 11H_2O$. Both minerals were formed as alteration products of As sulphides.

At Şaru Dornei, veins filled by calcite and realgar crosscut the black, poorly consolidated kaolinite-calcite-rich slate-like formation (Ghergari et al. 1992, Kristály & Szakáll 2009). Here, pharmacolite forms matted aggregates consisting of white, 0.5–2 mm long, elongated laths and acicular crystals with pearly lustre (*Figure 7*). Pharmacolite was formed by arsenate/calcite reactions during the acidic alteration of realgar. Gypsum is always a by-product of sulphate and calcite reactions, and, in a later stage, aragonite was also formed. X-ray powder diffraction data of pharmacolite are given in *Table XI.* The differences

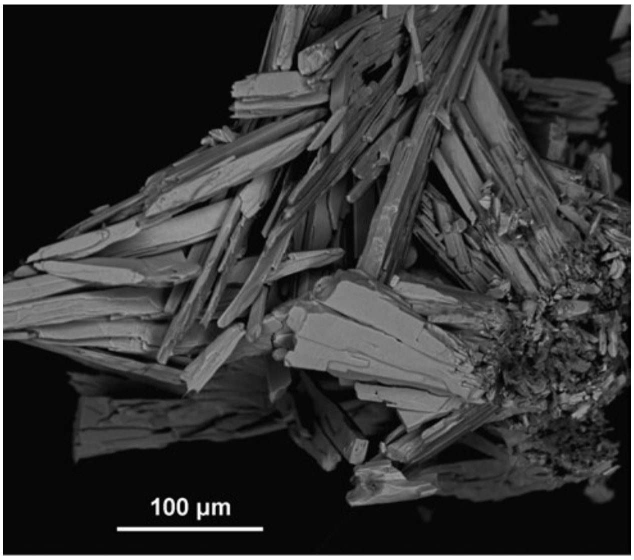

Figure 5. Prismatic pharmacolite crystals from Moldova Nouă. BSE image

5. ábra. *Farmakolit oszlopos kristályai. Újmoldova (Moldova Nouă), Románia. BSE-kép*

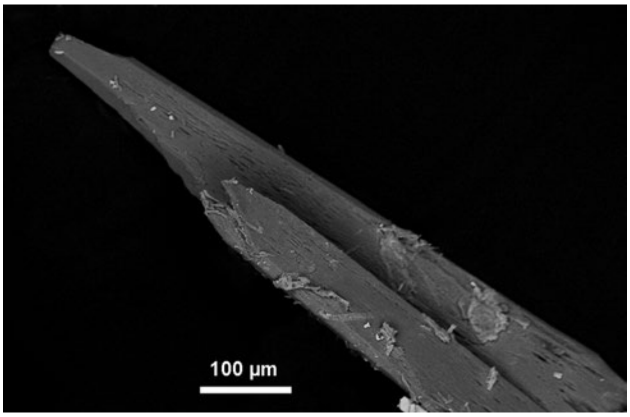

Figure 7. Lath-shaped pharmacolite crystal from Şaru Dornei. BSE image

7. ábra. *Léc alakú farmakolitkristály Sárosdornáról (Şaru Dornei). BSE-kép*

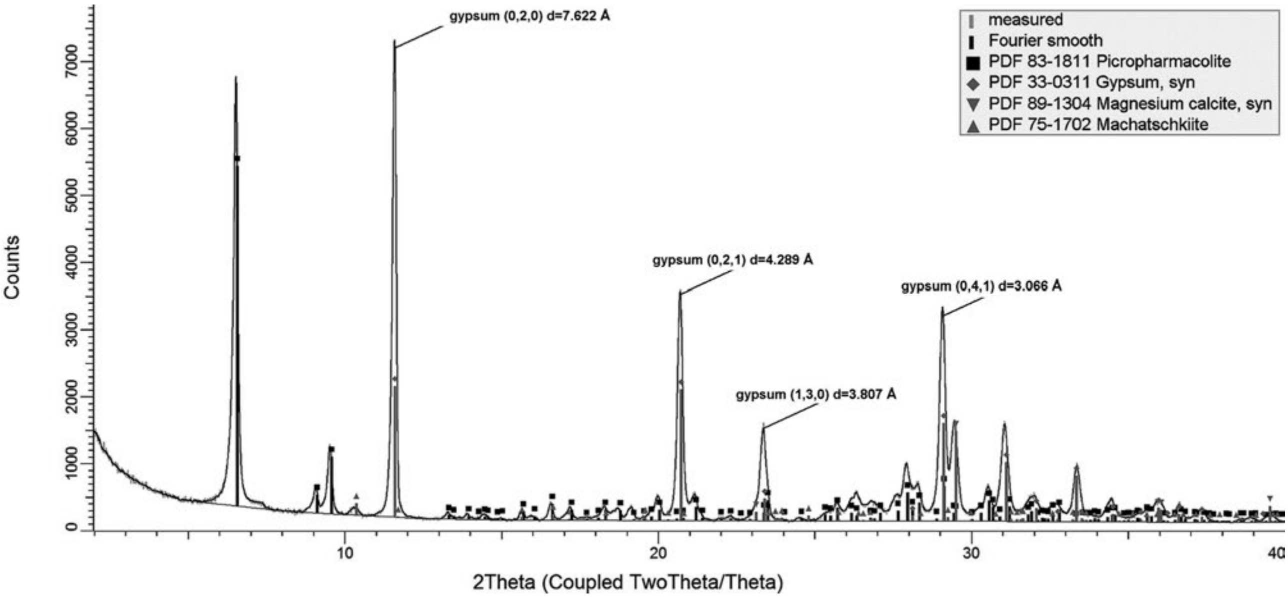

Figure 6. X-ray powder diffraction pattern of the picropharmacolite-bearing sample from Moldova Nouă

6. ábra. *Az újmoldovai (Moldova Nouă) pikrofarmakolit-tartalmú minta röntgen-pordiffrakciós felvétele*

Table XI. X-ray powder diffraction data of pharmacolite from Şaru Dornei compared with the data of the ICDD 00-074-0602 card

XI. táblázat. *A sárosdornai (Şaru Dornei) farmakolit röntgenpordiffrakciós adatai összehasonlítva az ICDD 00-074-0602 kártya adataival*

Pharmacolite Şaru Dornei		Pharmacolite (ICDD 00-074-0602) St. Andreasberg, Germany		
d (Å)	*I* (%)	*d* (Å)	*I* (%)	*hkl*
7.717	51.8	7.717	100.0	020
5.356	2.2	5.346	4.2	011
5.120	11.5	5.116	16.9	110
4.292	93.5	4.287	75.6	12-1
3.861	14.3	3.859	4.6	040
3.820	20.5	3.819	9.2	031
3.736	1.0	3.732	0.5	130
3.093	100.0	3.089	43.4	14-1
3.072	89.3	3.057	9.6	11-2
3.033	33.7	3.032	29.0	121
2.930	7.2	2.928	3.8	21-1
2.854	5.9	2.850	3.9	002
2.714	23.3	2.711	19.9	200, 051
2.707	26.8			
2.685	60.8	2.683	8.1	150
2.674	58.3	2.673	20.9	022
		2.667	13.8	13-2
2.585	3.9	2.578	5.6	20-2, 23-1
2.575	22.5	2.572	5.3	060
2.560	1.8	2.558	1.1	220
2.508	49.4	2.507	13.0	141
2.448	29.7	2.445	8.9	22-2
2.303	12.8	2.302	2.4	16-1
		2.292	1.4	042
2.221	26.2	2.218	7.5	240
2.217	23.4	2.194	2.0	15-2
2.150	1.7	2.153	0.5	112
2.144	2.2	2.143	1.0	24-2, 25-1
2.094	18.2	2.106	0.1	211
		2.056	0.1	071
2.042	2.9	2.042	0.2	170
2.028	5.8	2.028	0.8	161
2.017	15.5	2.015	5.1	12-3
2.004	2.1	2.003	0.4	132
1.995	3.0	1.983	0.7	21-3
1.965	6.0	1.965	0.9	231
1.930	31.2	1.929	2.2	080
		1.923	1.5	31-2
1.916	50.0	1.917	5.8	32-1
1.909	78.8	1.909	11.4	062
1.878	12.4	1.885	0.2	013
1.866	34.5	1.866	8.0	23-3, 260
1.837	42.4	1.836	7.2	14-3
1.822	56.2	1.821	7.7	26-2
1.815	20.7	1.814	4.3	33-2
1.808	19.2	1.807	2.0	18-1

between peak intensities of the measured and reference patterns are attributed to a contaminated sample, because our specimen mixed with calcite, kaolinite and realgar. The identification of pharmacolite is confirmed by the EDX spectrum (detection of Ca and As).

Slovakia

Hydrothermal tourmaline (magnesiofoitite) from Kapka locality, Remetské Hámre (Remetevasgyár)

Metasomatic bodies, formed by pneumatolytic-hydrothermal processes at the central part of the Vihorlat Mts., were described by BACSÓ (1971) and DERCO et al. (1977). The mineral paragenesis of the dominantly silicic alteration shows a well-defined zonation. The central zone consists of corundum, andalusite, topaz, tourmaline and clay minerals. The tourmaline is colourless or light blue, and it appears as minute needles or forms radial aggregates. According to BSE images, its chemical composition is homogeneous (*Figure 8*). Until now, the species-level determination of this tourmaline was impossible, due to the lack of chemical data. According to our results (*Table XII*), the dominant cations at

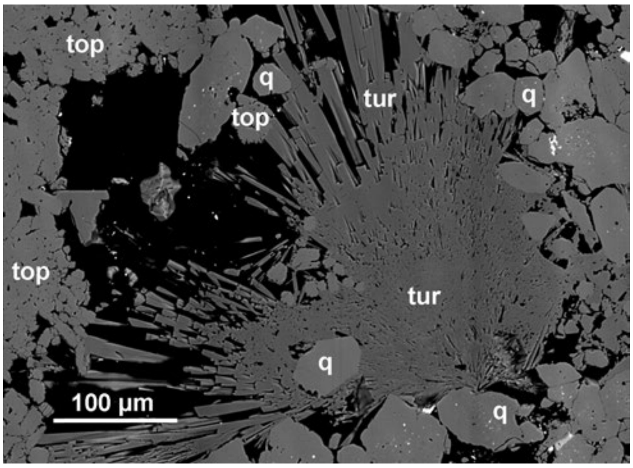

Figure 8. Radial aggregate of tourmaline (tur) with quartz (q) and topaz (top) from Kapka locality, Remetské Hámre. BSE image

8. ábra. *Turmalin (tur) sugaras halmaza kvarccal (q) és topázzal (top). Remetevasgyár (Remetské Hámre), Kapka lelőhely. BSE-kép*

Table XII. Electron-microprobe data of tourmaline from Kapka, Remetské Hámre (in wt%)

XII. táblázat. *A kapkai (Remetevasgyár, Remetské Hámre) turmalin elektronmikroszondás elemzési adatai tömegszázalékban*

SiO_2	37.71	37.57	36.24
TiO_2	0.05	0.00	0.01
B_2O_3*	11.21	11.21	11.09
Al_2O_3	40.92	40.92	41.75
FeO**	0.07	0.07	0.04
MgO	6.28	6.46	6.06
CaO	0.14	0.16	0.24
MnO	0.00	0.01	0.00
Na_2O	0.62	0.63	0.66
K_2O	0.03	0.03	0.02
F	0.01	0.00	0.00
H_2O*	3.86	3.87	3.83
-O=F	0.00	0.00	0.00
Total	100.90	100.92	99.93

Table XII. Continuation
XII. táblázat. *Folytatás*

Cation numbers based on 31 anions (O, OH, F) Kationszámok 31 anionra (O, OH, F)			
Si	5.846	5.826	5.681
Al	0.154	0.174	0.319
Σ*T*	**6.000**	**6.000**	**6.000**
B	**3.000**	**3.000**	**3.000**
Al	6.000	6.000	6.000
Σ*Z*	**6.000**	**6.000**	**6.000**
Al	1.323	1.306	1.395
Ti	0.006	0.000	0.001
Mg	1.451	1.494	1.416
Mn	0.000	0.001	0.000
Fe^{2+}	0.009	0.009	0.005
Σ*Y*	**2.790**	**2.810**	**2.818**
Ca	0.023	0.027	0.040
Na	0.186	0.189	0.201
K	0.006	0.006	0.004
[]	0.784	0.778	0.755
Σ*X*	**1.000**	**1.000**	**1.000**
OH	3.995	4.000	4.000
F	0.005	0.000	0.000

* Calculated from stoichiometry. / *A sztöchiometrikus összetételből számolva.*
** Total Fe was regarded as FeO. / *Az összes vasat FeO-ként vettük figyelembe.*

the different structural sites (for details see the subsection “Elbaite from the Darnózseli gravel pit”) are vacancy at the *X* site, Mg and Al at the *Y* site, Al at the *Z* site, Si at the *T* site and OH at both *V* and *W* sites. Based on the nomenclature of the tourmaline-supergroup minerals (HENRY et al. 2011), the Kapka tourmaline falls in the compositional field of magnesiofoitite.

Sodalite from alkaline basalts, Bulhary (Bolgárom)

The Bulhary maar/diatreme complex is built up from nepheline basanite with phenocrysts of olivine, clinopyroxene, plagioclase and rare opacitized amphibole. The volcano evolved in multiple (five) stages (KONEČNÝ & LEXA 2003). The formation of nepheline basanite sometimes rich in miarolitic cavities, was most probably connected to the second (laccolite-like intrusive body) stage of volcanism. In the first description of the cavity-filling mineral association by FARSANG et al. (2014), sodalite ($Na_8Al_6Si_6O_{24}Cl_2$) was mentioned as a rare phase (although no further details were given). During recent years, new specimens, rich in sodalite and leucite, have been found. Leucite forms white, 0.5–1 cm-sized unique, skeletal crystals, where only the edges of the trapezohedron have been developed. White and smaller sodalite crystals form 0.5–2-mm-sized rhombic dodecahedra. Its habit can be similar to that of leucite, namely ring-shaped skeletal or partially developed crystals, frequently with hollow faces (*Figure 9*). Some sodalite crystals are

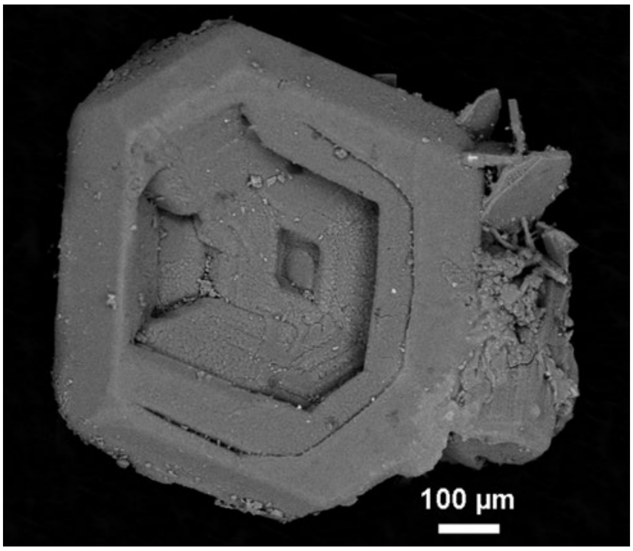

Figure 9. Skeletal crystal of sodalite from Bulhary. BSE image
9. ábra. *Szodalit vázkristály Bolgáromból (Bulhary). BSE-kép*

Table XIII. Electron-microprobe data of sodalite from Bulhary, Slovakia (in wt%)
XIII. táblázat. *A bolgáromi (Bulhary) szodalit elektronmikroszondás elemzési adatai tömegszázalékban*

SiO_2	37.90	37.96
TiO_2	0.01	0.02
Al_2O_3	30.06	30.77
Cr_2O_3	0.00	0.00
MgO	0.00	0.00
CaO	0.08	0.08
MnO	0.00	0.03
FeO	0.21	0.20
NiO	0.01	0.01
Na_2O	24.43	24.34
K_2O	0.03	0.04
F	0.00	0.00
Cl	7.34	7.40
-O=F, Cl	1.66	1.67
Total	98.41	99.18
Ion numbers based on 26 anions (O, Cl) Ionszámok 26 anionra (O, Cl)		
Si	6.19	6.15
Ti	0.00	0.00
Al	5.79	5.87
Cr	0.00	0.00
Mg	0.00	0.00
Ca	0.01	0.01
Mn	0.00	0.00
Fe	0.03	0.03
Ni	0.00	0.00
Na	7.74	7.64
K	0.01	0.01
O	23.97	23.97
F	0.00	0.00
Cl	2.03	2.03

perfectly developed combinations, although in some cases these latter ones can also be hollow inside. Besides the dominant rhombic dodecahedron, the cube and small faces of the octahedron and the trapezohedron have also been observed. There are well-developed minute crystals of magnetite, ilmenite, apatite, and titanite in close association with sodalite. According to the textural features observed in BSE images, sodalite can be consumed by the later formed leucite. Remnants of alkali feldspars are also present. The EPMA measurements data (*Table XIII*) are close to the sodalite ideal stoichiometric formula.

Sodalite with similar paragenesis and appearance is known from the Eifel region, Germany (HENTSCHEL 1987), and occasionally it has also been recorded in the cavities of basalt of Pauliberg, Austria (KOLITSCH et al. 2009).

Nickelhexahydrite and retgersite from Dobšiná (Dobsina)

Ni-Co sulphides and their secondary sulphates and arsenates are well known from the ore deposit of Dobšiná (MELCZER 1907, ĎUĎA & OZDÍN 2012). The re-investigation of the collection of Jenő RUFFINYI (a famous former director of the Dobšiná mine and discoverer of the Dobšiná ice cave) yielded some new Ni-Co-sulphide-rich ore specimens. Some of these are covered by a 2–3 mm-thick, porous crust on the surface consisting of secondary minerals.

Detailed investigation of these crusts has led to the identification of the following minerals: annabergite, erythrite, nickelhexahydrite, retgersite, gypsum and arsenolite. Of these, two Ni sulphates, nickelhexahydrite, ideally (Ni, Mg, Fe)$SO_4 \cdot 6H_2O$, and retgersite, ideally $NiSO_4 \cdot 6H_2O$, had not been identified from the locality earlier. Nickelhexahydrite forms light blue fibrous crusts or massive aggregates (*Figure 10)*. The rounded grains resemble euhedral crystals attacked by dissolution, in this case for example the humidity of the air. The irregularly cracked surface is also characteristic of the fast dehydration of highly hydrated materials. However XRD showed the presence of Ni substitution for Mg with variable ratios, as suggested by peak maxima falling between those of the hexahydrite and nickelhexahydrite species (*Table XIV*). Since zoning or any other pattern of Ni substitution is not observed on BSE images, it can be supposed that mixed Ni-Mg phases are present. The XRD data showed that hexahydrite also occurs, as observed on the powder pattern in *Figure 11, a*. Hydrotalcite is the product of hydrothermal processes; this affected the host rock, and led to the formation of the sulphate paragenesis. The presence of annabergite proves the existence of Ni-(sulph)arsenide phases prior to alteration. Retgersite forms ca. 1 mm-sized, green, pulverulent, irregular aggregates. Its X-ray diffraction pattern is given in *Figure 11, b*. Both Ni-sulphate minerals are well known from alteration zones of Ni sulphides, and can usually be found together (ANTHONY et al. 2003).

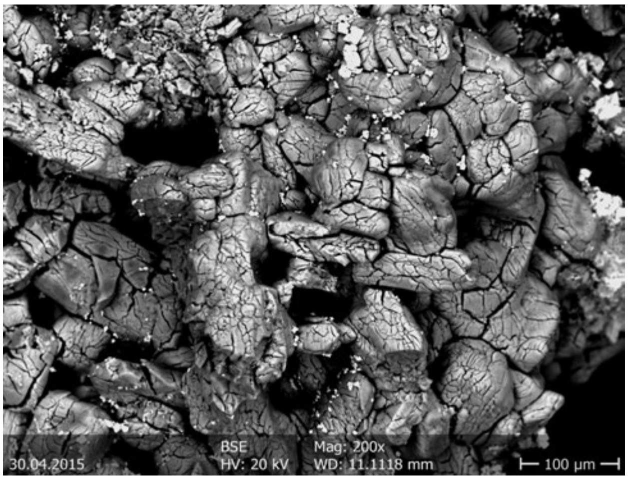

Figure 10. Crust-like aggregates of nickelhexahydrite from Dobšiná. BSE image

10. ábra. *Nikkelhexahidrit kéregszerű aggregátumai Dobsináról (Dobšiná). BSE-kép*

Table XIV. X-ray powder-diffraction data of nickelhexahydrite from Dobšiná compared with the corresponding reflections of the ICDD 00-033-0955 and 00-024-0719 cards

XIV. táblázat. *A dobsinai (Dobšiná) nikkelhexahidrit röntgen-pordiffrakciós adatai összehasonlítva az ICDD 00-033-0955 és 00-024-0719 kártyák megfelelő reflexióival*

Nickelhexahydrite Dobšiná		Nickelhexahydrite ICDD 00-033-0955			Hexahydrite ICDD 00-024-0719		
d(Å)	I(%)	d(Å)	I(%)	hkl	d(Å)	I(%)	hkl
		5.98	5	400	6.05	6	400
5.838	11	5.824	20	011	5.8	8	-111
		5.538	6	111	5.58	4	111
5.443	33	5.424	21	-211	5.45	50	-211
5.084	28	5.061	21	211	5.1	45	211
4.945	23	4.9	51	002, -311	5.01	4	002
4.839	26	4.782	24	-202	4.88	30	-202
4.543	6	4.519	6	311	4.56	8	311
4.384	100	4.367	100	-411	4.39	100	-411
		4.314	21	202			
4.135	14	4.096	22	-402	4.16	35	-402
4.021	48	4.003	60	411	4.04	45	411
		3.865	4	-511	3.893	10	-511
		3.625	14	020			
3.612	11				3.61	20	402
3.573	15	3.576	9	120	3.569	2	120
		3.544	20	402, 511			
		3.466	3	220			
3.452	9	3.432	8	-611	3.459	14	-611
3.373	7	3.34	8	-602	3.387	12	-602

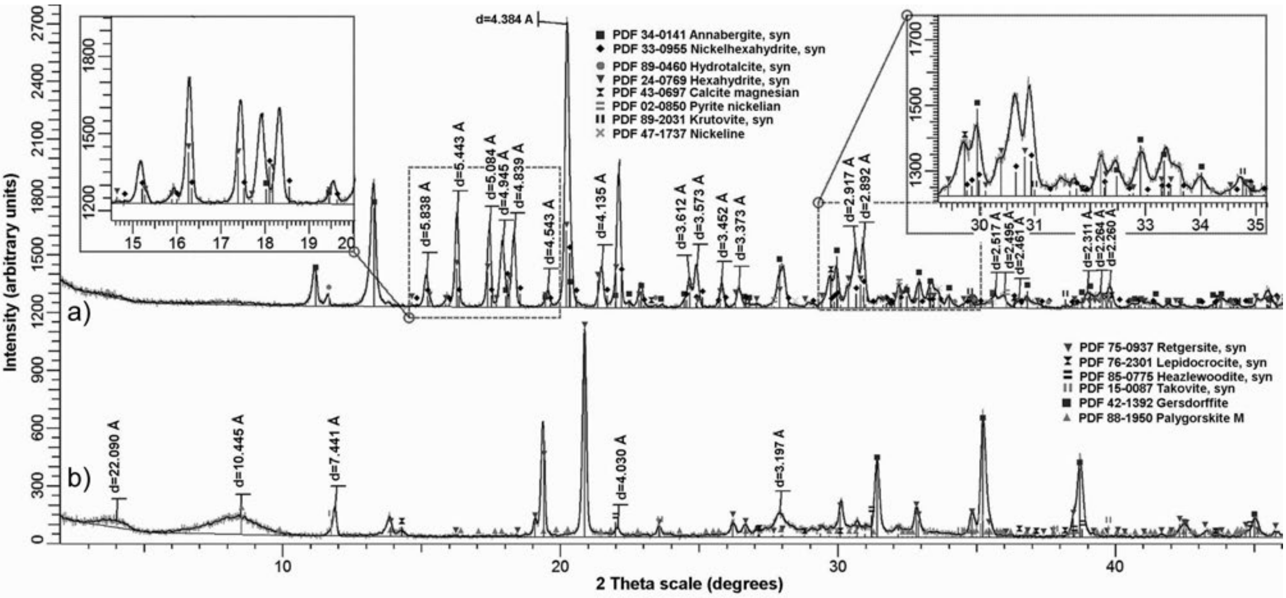

Figure 11. X-ray powder diffraction patterns of the nickelhexahydrite- (a) and the retgersite-containing (b) samples from Dobšiná

11. ábra. *A dobsinai (Dobšiná) nikkelhexahidrit- (a) és retgersittartalmú (b) minták röntgen-pordiffrakciós felvételei*

Acknowledgements

The authors are grateful to Michael NEUBAUER (Dobšiná) for the samples from the Ruffinyi-collection, Gábor KOLLER (Pilisborosjenő) for the arsenates from Moldova Nouă and Şaru Dornei and köttigite from Cârlibaba, Regina KÖRMENDY (Budapest) for the elbaite from Darnózseli, and finally to István HORVÁTH (Miskolc) for the zeolites from Alsótelekes. Both referees, Izabella FARKAS (MOL Group, Budapest) and Gábor PAPP (Hungarian Natural History Museum, Budapest) are highly acknowledged for comments and suggestions that helped to improve the manuscript.

This work was carried out as part of the TÁMOP-4.2.2.A-11/1/KONV -2012-0005 project, under the auspices of the Center of Excellence of Sustainable Resource Management, in the framework of the New Széchenyi Plan. The realization of this project was supported by the European Union, and cofinanced by the European Social Fund.

References — Irodalom

ANTHONY, J. W., BIDEAUX, R. A., BLADH, K. W. & NICHOLS, M. C. 2003: *Handbook of Mineralogy. Vol. V. Borates, carbonates, sulfates.* — Mineral Data Publishing, Tucson, 813 p.

BACSÓ, Z. 1971: Nové minerály a nové surovinové možnosti Vihorlatu (New minerals and raw material perspective in the Vihorlat Mts.). — *Mineralia Slovaca* **3/11,** 247–252 (in Slovak with English abstract).

DERCO, J., KOZÁČ, J. & OČENÁŠ, D. 1977: Nové poznatky o mineráloch a genéze sekundárnych kvarcitov lokality Kapka v centrálnom Vihorlate (New information about the mineralogy and genesis of secondary quartzites at Kapka locality in the central Vihorlat Mts. area). — *Mineralia Slovaca* **9/3**, 185–205 (in Slovak with English abstract).

ĎUĎA, R. & OZDÍN, D. 2012: *Minerály Slovenska [Minerals of Slovakia].* — Granit, Prague, 480 p. (in Slovak)

FARSANG, S., SZAKÁLL, S., OZDÍN, D., ZAJZON, N. & GAÁL, Ľ. 2014: A Cseres-hegység (Cerová vrchovina, Szlovákia) vulkanitjainak ásványai (Minerals of volcanites of the Cerová Highlands, Slovakia). — In: FEHÉR, B. (ed.): *Az ásványok vonzásában. Tanulmányok a 60 éves Szakáll Sándor tiszteletére (In the attraction of minerals. Studies in honour of the 60-year-old Sándor Szakáll).* Herman Ottó Múzeum & Magyar Minerofil Társaság, Miskolc, 27–43 (in Hungarian with English abstract).

GHERGARI, L., OLARU, G. & TRANDAFIR, V. 1992: Arsenic minerals at Şarul Dornei, Suceava region. — *Romanian Journal of Mineralogy* **75/1 (suppl.),** 12.

HENRY, D. J., NOVÁK, M., HAWTHORNE, F. C., ERTL, A., DUTROW, B. L., UHER, P. & PEZZOTTA, F. 2011: Nomenclature of the tourmaline-supergroup minerals. — *American Mineralogist* **96,** 895–913.

HENTSCHEL, G. 1987: *Die Mineralien der Eifelvulkane.* — Lapis Monographie, Weise Verlag, München. 176 p.

HOLLAND, T. J. B. & REDFERN, S. A. T. 1997: Unit cell refinement from powder diffraction data: the use of regression diagnostics. — *Mineralogical Magazine* **61,** 65–77.

JAMBOR, J. L. & DUTRIZAC, J. E. 1995: Solid solutions in the annabergite-erythrite-hörnesite synthetic system. — *Canadian Mineralogist* **33,** 1063–1071.

KOLITSCH, U., POSTL, W., BOJAR, H. P. & TRATTNER, W. 2009: Die Mineralvorkommen im Bazalt des Pauliberges. — In: GÖTZINGER, M. A. & HUBER, P. (eds): *Die Mineralien des Burgenlandes. Geologie, Mineralogie und mineralische Rohstoffe. Arbeiten aus dem Burgenland* Band **126,** Eisenstadt. 83–100.

KONEČNÝ, V. & LEXA, J. 2003: Evolution of the phreatomagmatic/extrusive/intrusive complex of the Bulhary maar-diatreme volcano in Southern Slovakia. — *Geolines* **15,** 47–51.

KRISTÁLY, F. & SZAKÁLL, S. 2009: Regional distribution of As-minerals on Neogene volcanic arc – cretaceous flysch boundary in the Romanian East Carpathians. — *Mitteilungen der Österreichischen Mineralogischen Gesellschaft* **155,** 94.

MELCZER, G. 1907: Gömörmegye ásványai [Minerals of Gömör county]. — In: EISELE, G. (ed.): *Gömör és Kishont törvényesen egyesült vármegyének bányászati monográfiája [Mining monography of Gömör and Kishont legally united counties].* Selmecbánya, Joerges Ágost özvegye és fia nyomdája, 521–546 (in Hungarian).

NOVÁK, M. & SELWAY, J. B. 1997: Locality No. 1. Rožná near Bystřice nad Pernštejnem, Hradisko hill. A large lepidolite subtype pegmatite dike. — In: NOVÁK, M. & SELWAY, J. B. (eds): *Tourmaline 1997 International Symposium on Tourmaline. Field trip guidebook.* Nové Město na Moravě, 23–38.

OLMI, F., SANTUCCI, A. & TROSTI-FERRONI, R. 1995: Sabelliite, a new copper-zinc arsenate-antimonate mineral from Sardinia, Italy. — *European Journal of Mineralogy* **7,** 1325–1330.

PAPP, F. & MÁNDY, T. 1955: Rézércnyomok Balatonfüreden (Traces of copper ore at Balatonfüred, Central Western Hungary). — *Földtani Közlöny* **85,** 457–459 (in Hungarian with English and Russian abstracts).

PASSAGLIA, E. 1970: The crystal chemistry of chabazites. — *American Mineralogist* **55,** 1278–1301.

RĂDULESCU, D. & DIMITRESCU, R. 1966: *Mineralogia topografică a Romăniei [Topographical mineralogy of Romania].* — Edit. Academiei, Bucureşti, 376 p. (in Romanian)

STURMAN, B. D. 1976: New data for köttigite and parasymplesite. — *Canadian Mineralogist* **14,** 437–441.

SZAKÁLL, S. & KRISTÁLY, F. (eds) 2010: *Mineralogy of Székelyland, Eastern Transylvania, Romania.* — Csík County Nature and Conservation Society, Sfântu Gheorghe-Miercurea Ciuc-Târgu Mureş. 321 p.

SZAKÁLL, S., FEHÉR, B., KRISTÁLY, F. & ZAJZON, N. 2013: Mineralogical mosaics from the Carpathian–Pannonian region 1. — *Földtani Közlöny* **143,** 177–187.

SZAKÁLL, S., FEHÉR, B., KRISTÁLY, F. & ZAJZON, N. 2014a: Mineralogical mosaics from the Carpathian–Pannonian region 2. — *Földtani Közlöny* **144,** 445–468.

SZAKÁLL, S., JÁGER, V., FEHÉR, B. & ZAJZON, N. 2014b: A mecseki fonolit ritkaföldfémtartalma és ásványi hordozói [Rare-earth content and its mineral carriers of phonolite of Mecsek Mts., Hungary]. — In: SZAKÁLL, S. (ed.): *Ritkaföldfémek magyarországi földtani képződményekben [Rare-earth elements in geological formations of Hungary].* CriticEl Monográfia 5. Milagrossa kft., Miskolc, 47–66 (in Hungarian)

TAKÉUCHI, Y., KUDOH, Y. & YAMANAKA, T. 1976: Crystal chemistry of the serandite-pectolite series and related minerals. — *American Mineralogist* **61,** 229–237.

ZAJZON, N., VÁCZI, T., FEHÉR, B., TAKÁCS, Á., SZAKÁLL, S. & WEISZBURG, T. G. 2013: Pyrophanite pseudomorphs after perovskite in Perkupa serpentinites (Hungary): a microtextural study and geological implications. — *Physics and Chemistry of Minerals* **40,** 611–623.

ZAJZON, N., SZENTPÉTERI, K., SZAKÁLL, S. & KRISTÁLY, F. 2015: The origin of the Avram Iancu U-Ni-Co-Bi-As mineralization, Băiţa (Bihor) metallogenic district, Bihor Mts., Romania. — *International Journal of Earth Sciences* **104,** 1865–1887.

ZELENKA, T., KALÓ, J. & NÉMETH, N. 2005: Az alsótelekesi gipsz-anhidrit dóm szerkezete (The structure of the gypsum-anhydrite dome at Alsótelekes). — *Földtani Közlöny* **135,** 493–511 (in Hungarian with English abstract).

ZEPHAROVICH, V. 1859: *Mineralogisches Lexicon für das Kaiserthum Österreich.* I. Band — Braumüller, Wien. 627 p.

Kézirat beérkezett: 2015. 06. 22.